Deformation Mechanisms in Nano-Crystalline Metals

by

Viswanath Raja Ramana Surya Ratna Chinthapenta

B.E.(Civil), Maturi Venkata Subba Rao College, Osmania University; India, 2003

M.E.(Aerospace), Indian Institute of Science; Bangalore, India, 2005

A dissertation submitted in partial fulfillment of the
requirements for the degree of Doctor of Philosophy
in The School of Engineering at Brown University

PROVIDENCE, RHODE ISLAND

May 2012

This dissertation by Viswanath Raja Ramana Surya Ratna Chinthapenta is accepted

in its present form

by The School of Engineering as satisfying the

dissertation requirement for the degree of Doctor of Philosophy.

Date_____ _____

Allan Francis Bower, Ph.D., Advisor

Recommended to the Graduate Council

Date_____ _____

Kyung-Suk Kim, Ph.D., Reader

Date_____ _____

K Sharvan Kumar, Ph.D., Reader

Approved by the Graduate Council

Date_____ _____

Peter M. Weber, Dean of the Graduate School

Vitae

Acknowledgements

Abstract of "Deformation Mechanisms in Nano-Crystalline Metals" by Viswanath Raja Ramana Surya Ratna Chinthapenta, Ph.D., Brown University, May 2012

Contents

List of Tables

List of Figures

Chapter 1

Mechanics of FCC Nano-Crystalline Metals

Chapter 2

Deformation Mechanisms in FCC Nano-Crystalline Metals

Chapter 3

Continuum Modelling of Polycrystalline Metals

Chapter 4

Intergranular Strain Evolution

Chapter 5

Meso-scale Modelling of Polycrystalline Metals

Chapter 6

Dislocation-Dislocation Interactions: N Particle Problem

Dislocation is a defect in crystal. It was independently proposed by Orowan [**?**], Polanyi [**?**] and Taylor [**?**] in 1934. Dislocations are difficult to observe, but in 1939 Burgers [**?**] has come up with the concept of failure of circuit close that is drawn around material containing a dislocation. This closure failure (displacement discontinuity) is defined as Burgers vector $\underline{b}$.

$$\underline{b} = b_1\underline{e}_1 + b_2\underline{e}_2 + b_3\underline{e}_3 \tag{6.1}$$

Before we go further we list out the dislocation conventions (sense) used in here, unless other specified these convention applied throughout. Burgers vector that is drawn around a prefect crystal in a cloclwise direction yields no closure failure. When the same Burgers circuit is drawn clockwise direction around the dislocation with the dislocation line direction pointing in to the plane of the paper leads to a clousre failure. This closure failure is the vector joining the finish to start of the Burgers circuit.

Based on the components of Burgers vector, dislocations are classified into three types and those are screw, edge and mixed type. For a screw dislocation the non zeros Burgers vector components is only the out of plane component ($b_1 = 0$, $b_2 = 0$, $b_3 \neq= 0$). The sense of the screw dislocations are shown in the Fig. **??**. Similarly, for the edge dislocation atleast one of the in plane components of the Burgers vector is non zero and the out-of-plane component is zero. The sense of the edge dislocation are shown in the Fig. **??**. Finally, when both the in-plane and out-of-plane components of the Burgers vector are nonzero it is classified as mixed type.

Figure 6.1

It is worth to note that dislocation line cannot start and end inside the material. Lets assume it ends inside the material then if we traverse along the dislocation line we have a displacement discontinuity equal to Burgers and when we reach the same point from the prefect crystal there is none which contradicts each other and hence dislocation cannot either start or end inside a material. While it can be a circular dislocation (any closed loop) or it should start and end outside the material. In our study we limit our study to 2D straight dislocations.

6.1 Dislocation: A fundamental unit of plasticity

Dislocation can move by glide along the closed packed direction on the slip plane or can climb. Dislocation glide is stress assisted phenomenon where as climb has to be further assisted by the vacancy diffusion mechanism and its a thermal process. We restrict dislocation motion to glide mechanism since we focus our study on athermal processes.

The motion of dislocation is point of interest because in a perfect crystal a stress of the order of $\mu/3$ (nearly Theoretical bond-strength) is required to move atoms in the materials. But, in the presence of dislocation the atoms can be easily moved [**?**, **?**] and of the order of the shear strength observed experimentally.

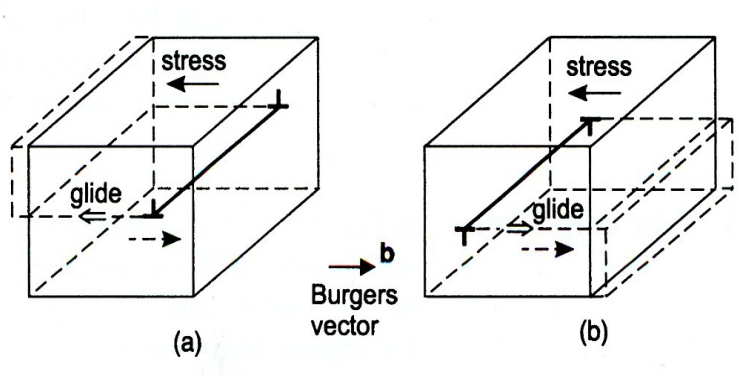

Figure 6.2: Plastic deformation by glide of edge dislocation under applied shear stress (a) Positive edge dislocation (b) Negatice edge dislocation [**?**]. As a result of edge dislocation gilde a step is formed along the dislocation line at the end of the block.

Consider two edge dislocations of opposite sign gliding on the slip plane. Steps are formed on the either side of the material as the dislocations pass out of the material as shown in the Fig. **??**. Similarly, also consider two screw dislocation of opposite sign. As the screw dislocations pass out of material steps are formed along the length of the plane of the paper on either side of the block as shown in the Fig. **??**. Hence as a result of motion of dislocation material undergoes plastic deformation. Since we only focus on the 2D problems the plastic deformation due to edge dislocation is only of our interest.

In this next two section we briefly describe the 2D discrete dislocation mechanics and 2D modelling. We follow the formulation of the Vander Giessen et al . [**?**]. For a detailed review follow the references [**?**, **?**].

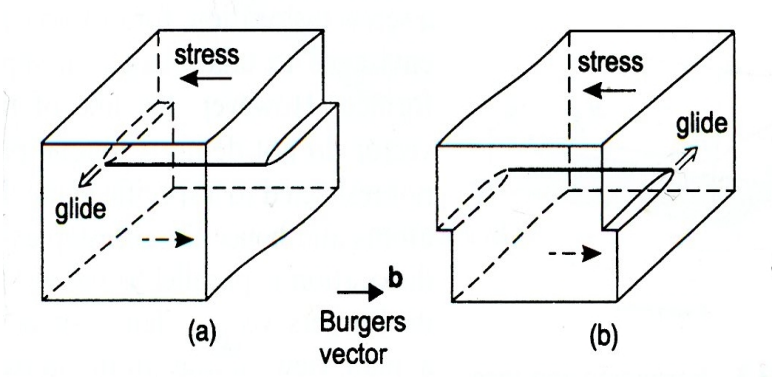

Figure 6.3: Plastic deformation by glide of screw dislocation under applied shear stress (a) Positive screw dislocation (b) Negatice screw dislocation [**?**]. As a result of screw dislocation glide a step is formed perpendicular to the dislocation line at the end of the block.

6.2 2D Discrete dislocation mechanics

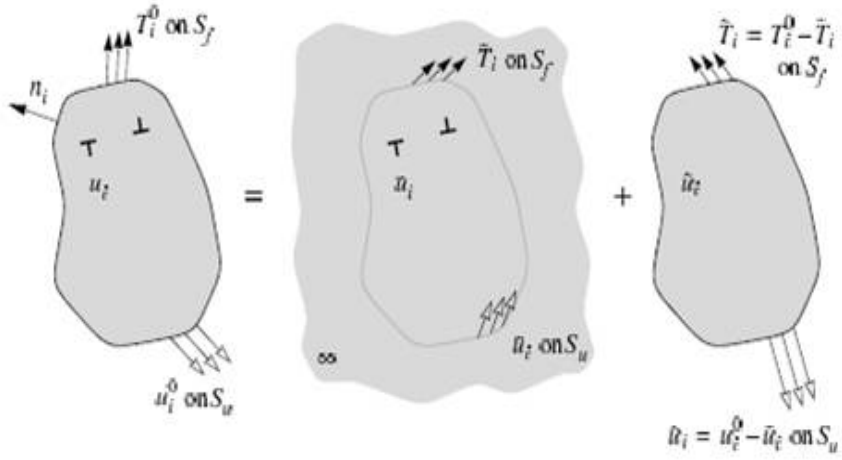

Figure 6.4: Decomposition into the problem of interacting dislocations in the infinite solid ($\tilde{}$ fields) and the complementary problem for the finite body without dislocations ($\hat{}$ fields) [**?**, **?**] .

We now present the Vander Giessen et al. [**?**] formulation for determing the mechanical fields in an arbitrary dislocated body subjected to the arbitrary boundary conditions. As shown in the Fig. **??** the problem can be divided into $\tilde{()}$ the fields due

to dislocations fields in an infinite space and $\hat{()}$ corrected field for the proper boundary conditions. That is the displacement, strain and stress fields are decomposed as

$$u_i = \tilde{u}_i + \hat{u}_i \tag{6.2}$$

$$\epsilon_{ij} = \tilde{\epsilon}_{ij} + \hat{\epsilon}_{ij} \tag{6.3}$$

$$\sigma_{ij} = \tilde{\sigma}_{ij} + \hat{\sigma}_{ij} \tag{6.4}$$

$$\tag{6.5}$$

The $\tilde{()}$ fields are the superposition of the singular fields of the dislocations in their-current configuration, but in infinte space. Identifying the fields for dislocations k by a superscript (k), the stress $\tilde{()}$ stress field, for example, is obtained as $\tilde{\sigma}_{ij} = \Sigma_k \sigma_{ij}^{(k)}$. The actual boundary conditions, interms of prescribed displacement u_i^0 or tractions $T_i^0 = \sigma_{ij} n_j$, are imposed through the $\hat{()}$ fields, in such a way that the sum of the $\tilde{()}$ and $\hat{()}$ fields in (Eq. **??**) gives the solution that satisifies all boundary conditions. It is important to note that the solution of the $\hat{()}$ problem deos not involve any dislocations and are smooth, so can be solved using a finite element method.

6.3 Discrete dislocation 2D-modeling

Density (ρ) : Dislocation density is defined as the total length of dislocation line per unit volume of crystal. In 2D modelling with all straight dislocations parallel to each other $\rho = 1/A$, where A is the area of the simulation cell. In a well annealed crystals the dislocation desity is of the order $10^{10} - 10^{12}$ m^{-2}. The dislocation density evolves and increases with the plastic deformation.

Interaction: Dislocation causes highly non-linear distribution of displacements in its vicinity, but beyond the dislocation core 10-12b it causes a residual elastic field which decay as $1/r$. As a result each dislocation interacts elastically with all other dislocation, which are sufficently far from the dislocation core. Since $1/r$ is a slow decay these interaction are long range interactions. Hence the Peach-Koehler ($f^{(k)}$) on dislocation k can be expressed as

$$f^{(k)} = n_i^{(k)} \left(\hat{\sigma}_{ij} + \Sigma_{l \neq k} \sigma_{ij}^{(l)} \right) b_j^{(k)} \tag{6.6}$$

Where $\hat{\sigma}_{ij}$ is the image stress (see Sec. **??**), $\sigma_{ij}^{(l)}$ is the interaction stress due to dislocation (l) on dislocation (k) and $b_j^{(k)}$ is Burgers vector of dislocation (k). *Mobility:* Dislocation glide is a complex phenomenon involving the viscous drag due to interactions with electrons and phonons. Ignoring the inertial effects the drag force can be expressed as

$$f^{(k)} = B v^{(k)} \tag{6.7}$$

Nucleation : Frank-Read source nucleates new disocation pair. The operation of Frank-Read source is shown in Fig. **??**. The intial dislocation segement of a Frank-Read source bows out due to resolved shear stress on the dislocation segment. The bowing out dislocation segement produces a new dislocation loop and replicate itself. The Frank-Read source is characterized by a critical value of Peach-Koehler force, the time it takes to generate a loop and the size of the generated loop. In 2D-modelling Frank-Read source is simulated by a point source generating a dislocation dipole when the magnitude of Peach-Koheler exceeds the source strength ($\tau_{nuc} b$) during a nucleation time t_{nuc}. The dislocation dipole is seperated by L_{nuc} so that the dipole does not collapse onto itself under an applied force of $\tau_{nuc} b$ as shown in Fig. **??**. The polarity

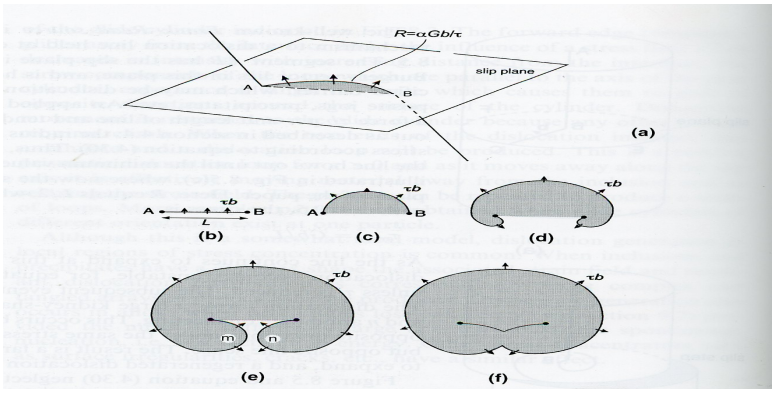

Figure 6.5

of the new dipole genrated is decided by the sign of the τ. The distance L_{nuc} between

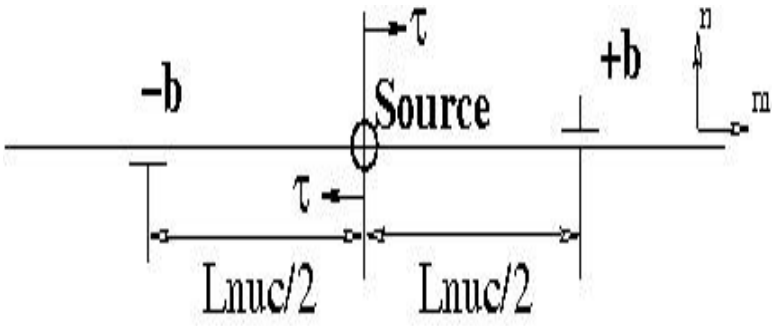

Figure 6.6

the two dislocations is determined by the critical stress which enusres that, when the new dipole is generated, the total resolved shear stress balances the attractive shear stress that the two dislocations exert on one another.

$$L_{nuc} = \frac{\mu}{2\pi(1-\nu)}\frac{b}{2\pi} \tag{6.8}$$

Annihilation : Annihilation of two dislocations with opposite Burgers vector occurs when they are sufficiently close together. Which is modelled by eliminating the two

opposite dislocation on same slip plane when they are within a material dependent, critical annihilation distance $L_{ann} \sim 6 - 10b$ as shown in Fig. **??**.

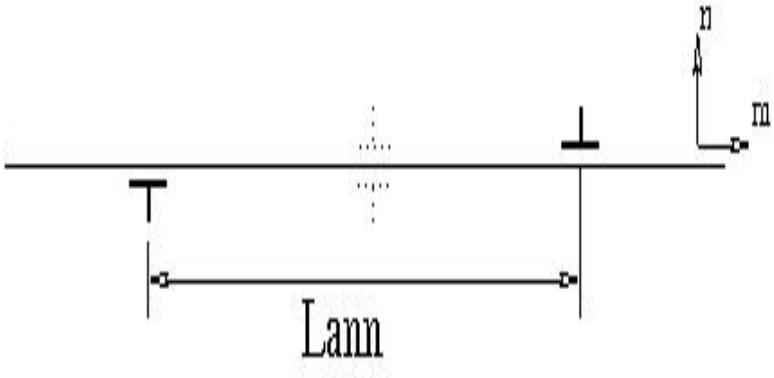

Figure 6.7

Obstacles and pile-up : Obstacles are modelled as passing and non-passing obstacles, where the former has the finite strength $\tau_{obs}b$ and the later has infinite strength. Obstacles are modelled as the fixed points on the slip plane. These fixed points causes pile up of dislocations. When the Peach-Koheler force on the leading dislocation of the pile up exceeds the obstacle strength the pinned dislocation against the obstacle is allowed to pass over the obstacle as shown in the Fig. **??**.

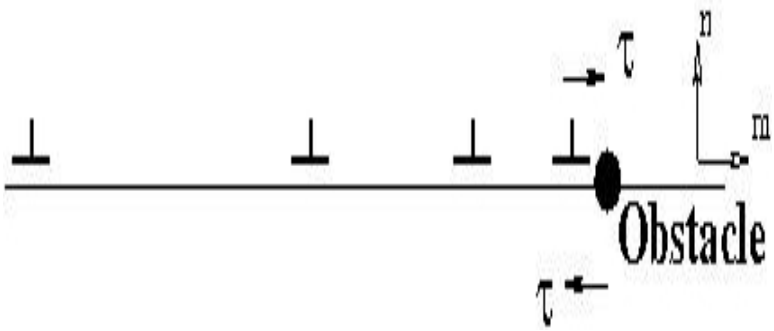

Figure 6.8

6.4 Bottle necks in discrete dislocation simulations

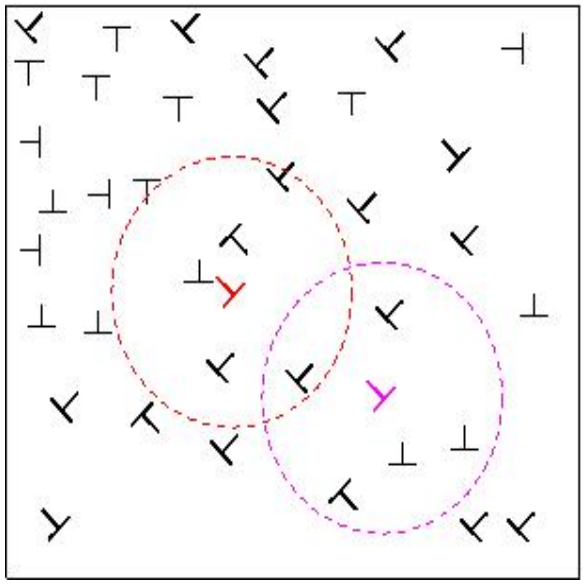

Figure 6.9

6.5 Complex potentials of 2D edge and screw dislocations

Screw : Potential for an isolated straight screw-dislocation at orgin in an infinite solid with line direction $\underline{t} = \underline{e}_3$.

$$\Theta(z) = \frac{-i\mu b_3}{2\pi}\, log(z) \tag{6.9}$$

Where μ is the shear modulus, b_3 is the Burgers magnitude (screw-component). *Edge :* Potentials for an isolated straight edge-dislocation at orgin in an infinite solid with

line direction $\underline{t} = \underline{e}_3$.

$$\Omega_o(z) = -i\frac{E(b_1 + ib_2)}{8\pi(1-\nu^2)}\, log(z) \tag{6.10}$$

$$\omega_o(z) = i\frac{E(b_1 - ib_2)}{8\pi(1-\nu^2)}\, log(z) \tag{6.11}$$

Where E is the elastic modulus, b_1 and b_2 are the Burgers components (edge-components) and ν is Poisson's ratio.

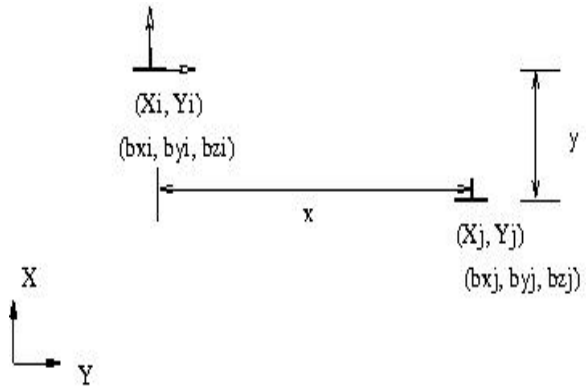

Figure 6.10

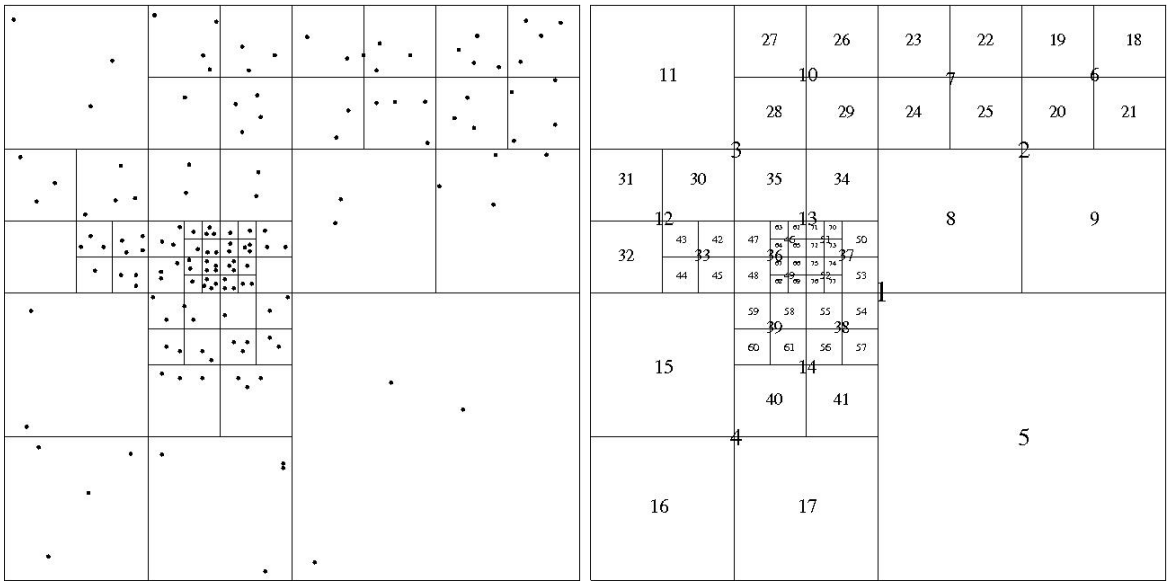

Figure 6.11

6.6 Dislocation dislocation-wall interactions

6.7 Doubly period dislocation-dislcoation interactions

6.8 Dislocation-Dislocation Interaction

6.9 Direct method

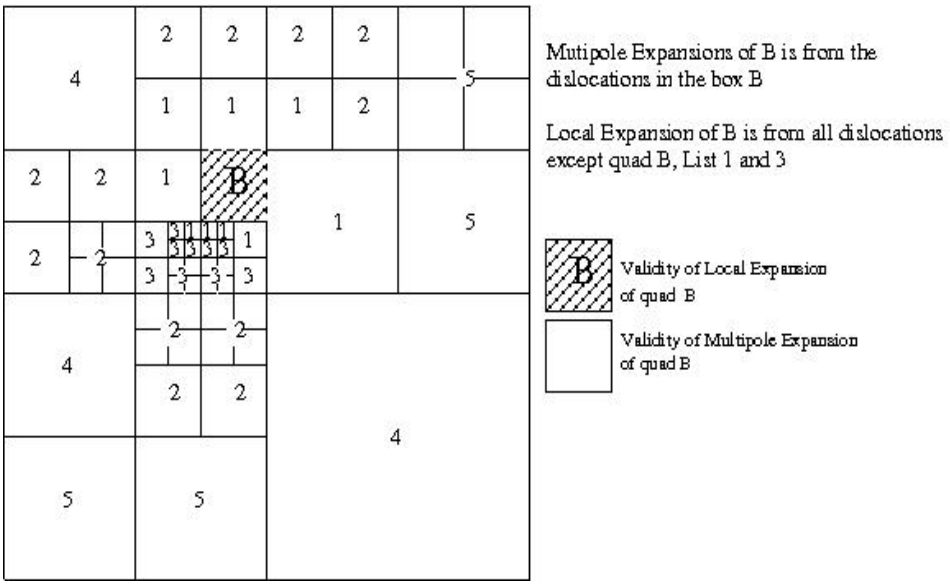

Figure 6.12

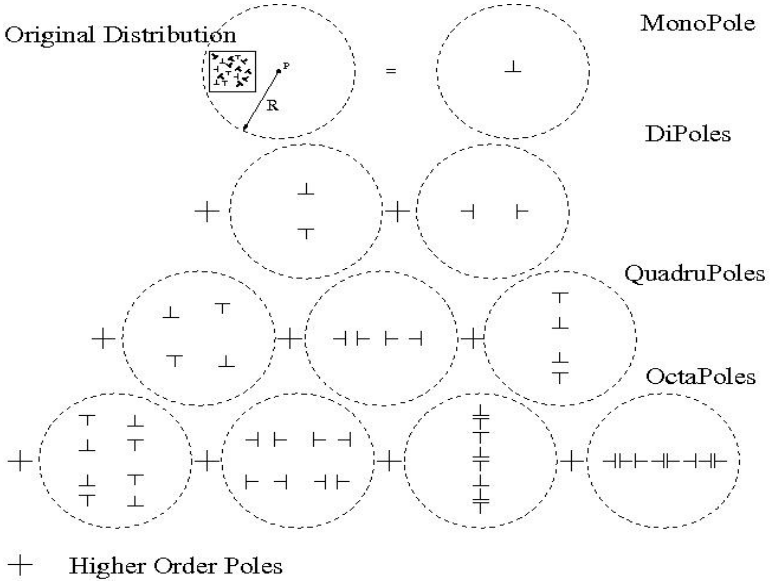

Figure 6.13

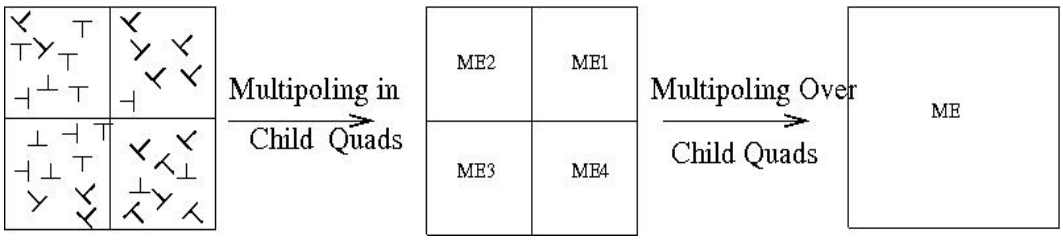

Figure 6.14

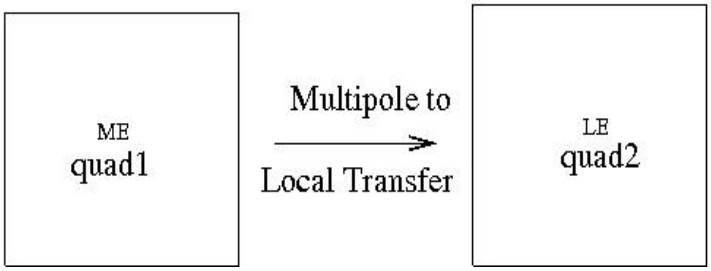

Figure 6.15

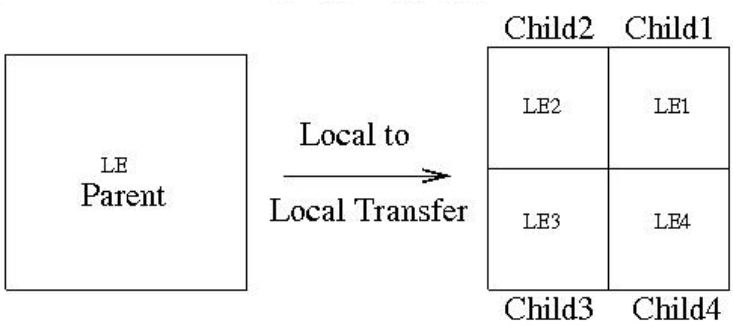

Figure 6.16

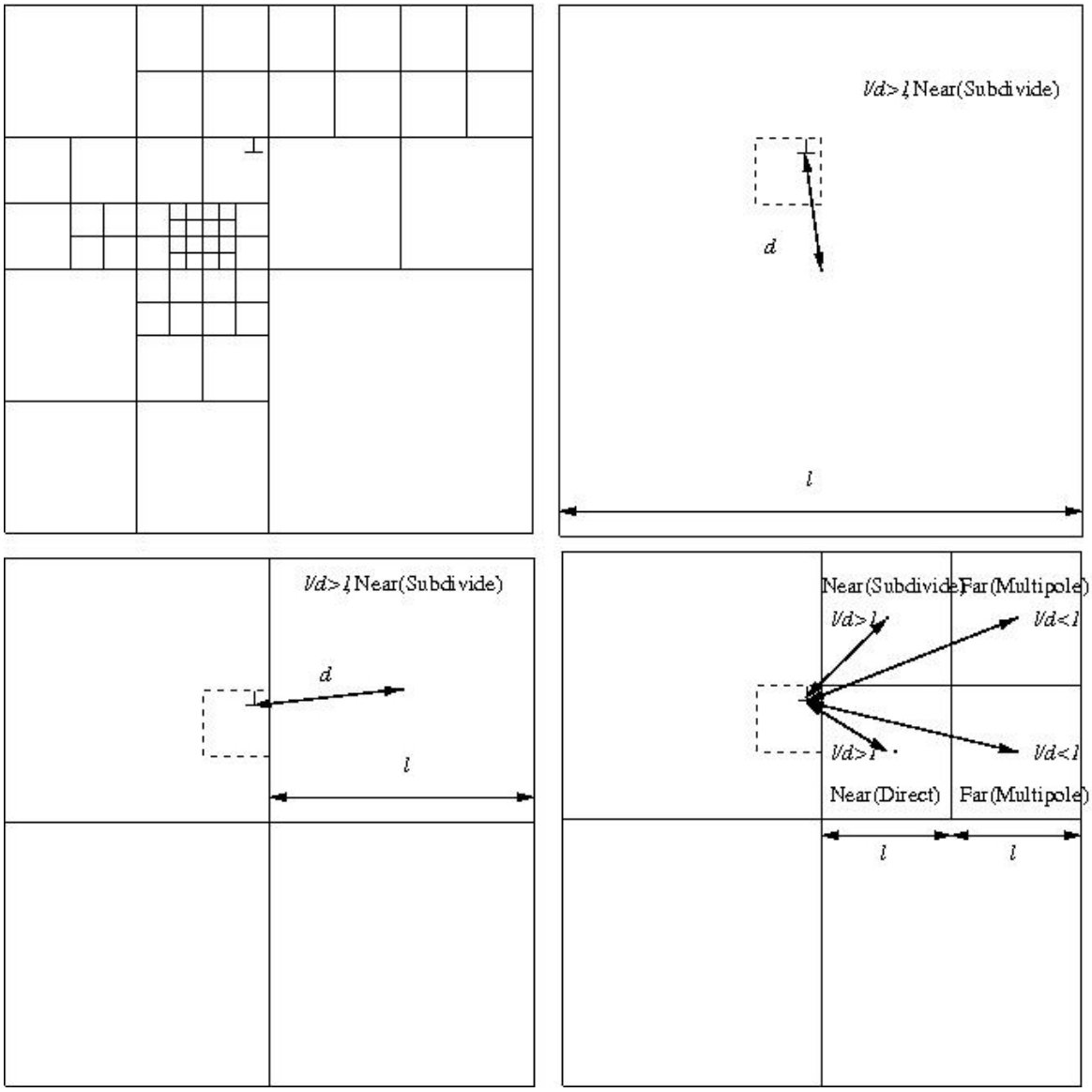
l/d>1, Near(Subdivide)
d
l
l/d>1, Near(Subdivide)
d
l
Near(Subdivide)
Far(Multipole)
l/d>1
l/d<1
l/d>1
l/d<1
Near(Direct)
Far(Multipole)
l
l

Figure 6.17

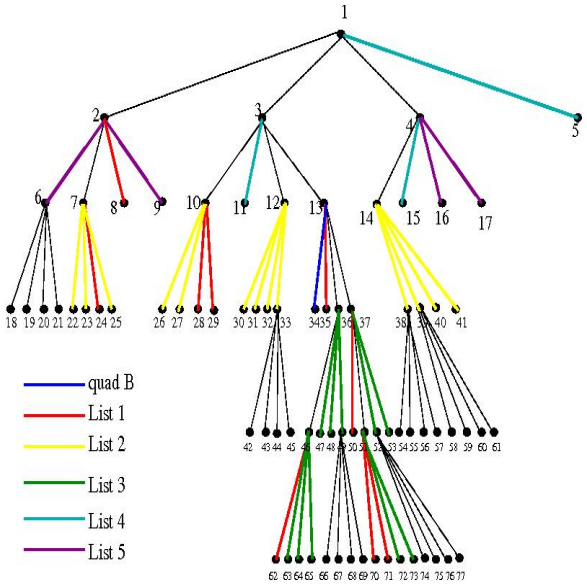

Figure 6.18

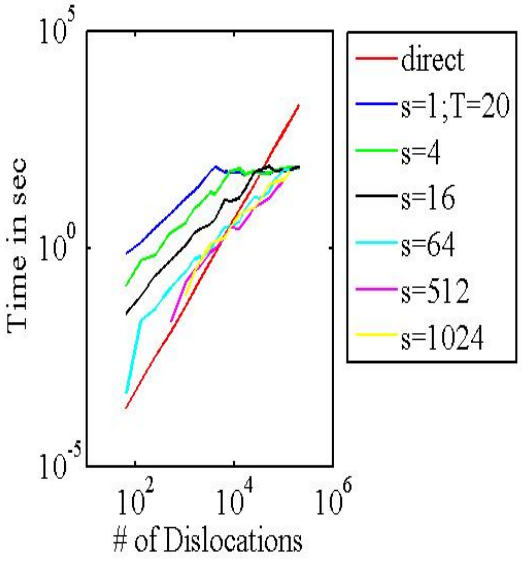

Figure 6.19

Chapter 7

Conclusion and Perspective

7.1 Concluding remarks

Evolution of lattice and intergranular strain gives measure of plastic and elastic anisotropy. Which are used to identify underlying deformation mechanisms.

- In dislocation dominated regimes most of the reflections.
- Intergranular in mixed deformation exhibits shift in the order of reflections indicating competition in deformation regime.
- Complete shift from dislocation dominated regime to GB mediated plasticity is due to loosing plastic anisotropy. This is shown during evolution of lattice strain in GB mediated plasticity regime. And through the stress computation in hexagonal grains.

- At the onset of mixed regime and at partial-Full cross over a sudden change in plastic anisotropy is observed . Indicating that intergranular can be used to detect the presence of partials.
- Grain interactions studies are carried out which are difficult to be undertaken by either atomistics or mechanistic methods using continuum techniques.
- The interaction studies demonstrate the peak broadening indicating the presence of dislocation activity in dislocation dominated and mixed regime.

In another studies related to development of mechanistic modelling, We crossed one of the major bottleneck by implementing the fast adaptive multipole-multipole method.

7.2 Outlook of future research

The present understanding of deformation mechanism through intergranular strain and grain interaction studies can be further extended to understand the grain level hetrogenities to understand the origins of microstress. But current experimental advancement limits such an approach.

In the Discrete dislocation modelling we have reached considerable advancement by fast interaction computations and modelling the boundary conditions to some extent. The has to further address the numerical instabilities and benchmarking to make into functional form.